IOP Conference Series: Materials Science and Engineering

PAPER • OPEN ACCESS

# An analytical model for predicting the extrusion force for the torsion extrusion process of metals

To cite this article: Z Y Liu *et al* 2022 *IOP Conf. Ser.: Mater. Sci. Eng.* **1270** 012075

# An analytical model for predicting the extrusion force for the torsion extrusion process of metals

**Z Y Liu[1,2], S L Zhao[1,2] and Z S Cui[1,2]**
[1] School of Materials Science and Engineering, Shanghai Jiao Tong University, 800 Dongchuan Road, Shanghai, 200240, P.R. China
[2] Institute of Forming Technology & Equipment, Shanghai Jiao Tong University, 1954 Huashan Road, Shanghai, 200030, P.R. China

**Abstract.** Torsion extrusion (TE) method as a severe plastic deformation (SPD) process can effectively refine the microstructures and improve the mechanical properties of materials. Accurate and rapid prediction of the extrusion force in the process of TE is an important problem in industry. This paper proposed an analytical model using upper bound method (UBM) for predicting the extrusion force in the TE process. The kinematically admissible velocity field is established based on a continuous spherical extrusion velocity field coupled with a torsional velocity field constrained in a conical die. The torsional angular velocities along the radial and axial directions are assumed with quadratic and cubic function, respectively, due to the radial and axial nonlinearity of torsional velocity in the deformation zone. In addition, considering its complexity, the shape of the deformation zone is mapped to a rectangular zone. By establishing the torsional velocity field in the mapped zone, the torsional velocity field of the deformation zone is obtained according to the mapping relation. The UBM model is validated by comparing the predicted extrusion force with the simulation results obtained from the finite-element method (FEM). Moreover, the influences of the friction factor, reduction ratio and die angle on the extrusion force were investigated as well.
**Keywords.** torsion extrusion; extrusion force; upper bound method

## 1. Introduction

Processing through severe plastic deformation (SPD) has now accepted widely as a promising tool for the fabrication of bulk ultrafine-grained (UFG) materials [1]. Different SPD techniques have been proposed such as equal-channel angular pressing (ECAP) [3], high pressure torsion (HPT) [4], accumulative roll-bonding (ARB) [5] and friction stir processing (FSP) [6]. However, these methods have great challenges in industrial application due to the low process efficiency, the complexity and the limited product size. Therefore, a new SPD process called torsion extrusion (TE) has been proposed for the industrialization of SPD methods [7].

In the TE process, the extrusion is assisted by a rotation imposed on the extrusion die, which produces the severe shear deformation to the extruded materials. Many researches have been carried out recently to this new process, both in the deformation mechanism and in the characterization of extruded materials. However, due to its complexity, very few analytical models and solutions can be found in the literature related with TE. Brovman et al [8] obtained an analytical model of extrusion force based on stress analysis for material flow through a rotating conical die excluding the circumferential slipping effect. Ma et al [9] analyzed the forming process of extrusion through steadily rotating die, theoretically and experimentally. They suggested a velocity field in the spherical coordinate system for material flow based on the simple elasticity theory and deduced the analytical model of extrusion force by using the

IOP Conf. Series: Materials Science and Engineering 1270 (2022) 012075 doi:10.1088/1757-899X/1270/1/012075

upper bound method. They inspected the effect of slippage factor and semi-die angle in extrusion pressure and finally determined the optimum die angle. Maciejewski and Mróz [11] analyzed the axisymmetric extrusion process with cyclic torsion by applying upper bound method. The evolution of the extrusion force and torsional moment was studied with process parameters such as the ratio of extrusion and rotation rates as well as the amplitude of die rotation. Although the above models can predict the extrusion force for TE, due to the great simplification of velocity field assumption, they are difficult to accurately predict the metal flow.

In the present paper, an analytical model for predicting the extrusion force in the TE process will be proposed by applying UBM. The kinematically admissible velocity field is established based on a continuous spherical extrusion velocity field coupled with a torsional velocity field constrained in a conical die. The UBM model is validated by comparing the predicted extrusion force with the simulation results obtained from the FEM. Then the influences of the friction factor, reduction ratio and die angle on the extrusion force are investigated.

## 2. Analytical model

### *2.1. Process principle*

In the torsion extrusion process, the container is stationary, and the rotating die drives billet to rotate. According to the deformation characteristics, the billet can be divided into three zones (I, II and III) as shown in figure 1. In the process, a cylindrical billet with an initial radius of $R_0$ is extruded through a conical die with an opening angle of $2\alpha$ , and is extruded to a final radius of $R_1$ . At the entrance of the die, the billet travels with an axial velocity of $\dot{u}_0$ parallel to the extruding direction. The extruded billet moves as a rigid body with an axial velocity of $\dot{u}_1$ . The rotating die rotates at the angular velocity $\omega_d$ . In this deformation mode, the velocity discontinuity is assumed existing on $S_2$ and $S_3$ , which stand for the boundaries between zones I and II, and zones I and III, respectively.

As shown in figure 2, the rotating die rotates at the input angular velocity, and the billet is driven to rotate by the friction of the rotating die. However, because of the circumferential slippage between the rotating die and billet, the billet rotates with a lower angular velocity than the rotating die. According to the deformation characteristics, the angular velocity of billet gradually decreases from the exit to the entrance of conical die in the axis direction, and the angular velocity of billet gradually decreases from the outer surface to the center in the radial direction. In zone II, there is always friction at the interface of the container and billet, Therefore, it is known that this friction prevents the billet slipping against the container. Under this condition, the angular velocity of billet gradually decreases to zero from the entrance of the rotating die to the punch.

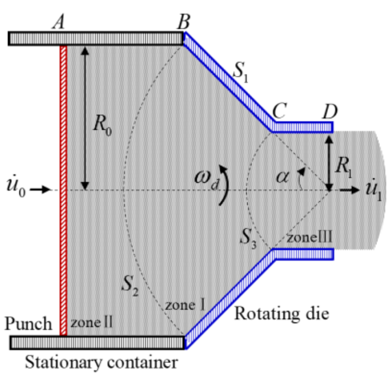


**Figure 1.** Schematic representation of TE process.

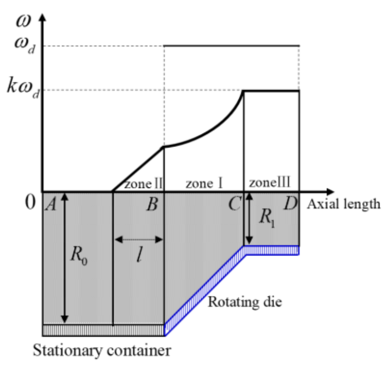


**Figure 2.** The distribution of rotating angular velocity of billet at the outside surface.

IOP Conf. Series: Materials Science and Engineering 1270 (2022) 012075 doi:10.1088/1757-899X/1270/1/012075

*2.2. Basic assumptions*

To analyze the torsion extrusion process by upper bound method, a proper kinematically admissible velocity field is deemed essential to ensure the accuracy of the final solution. In the deformation zone I, the velocity caused by the punch can be established by the incompressible requirement and boundary condition. But the velocity resulted from the rotating die is very complex. Because of the circumferential slippage between the rotating die and billet, the billet in the zone III rotates at a lower angular velocity compared to the rotating die. A circumferential slippage parameter *k* (angular velocity ratio of the billet at exit of conical die to rotating die) is applied to describe this difference. To simplify the nonlinearity of torsional velocity in the deformation zone I, it is assumed to be distributed as quadratic function along the radial direction and cubic function along the axial direction. A length *l*, which denotes the twisting length of billet in the zone II, is also assumed and it depends on the friction of the billet with the container surface.

Therefore, the rotating angular velocity of different zones of billet can be assumed as follows:

(I) The angular velocity of billet in rotating die is:

$$\begin{aligned} \omega_{\mathrm{c}} &= k\omega_{\mathrm{d}} \\ \omega_{R_x} &= c_0 + c_1 x + c_2 x^2 + c_2 x^3 \\ \omega_y &= m_0 + m_1 y + m_2 y^2 \end{aligned} \tag{1}$$

where $\omega_d$ is the constant angular velocity of the die, $\omega_c$ is the angular velocity of billet outer surface at the exit of rotating die, $\omega_{R_x}$ is the angular velocity of billet outer surface inside rotating die, $\omega_y$ is the radial angular velocity of the billet inside rotating die, the $k$ is the circumferential slippage parameter, the $m_0$, $m_1$, $m_2$, $c_0$, $c_1$, $c_2$ and $c_3$ are undetermined coefficient, $x$, $y$ are the radial and axial coordinates in the Cartesian coordinate system, which can be shown in the figure 3.

(II) The rotating angular velocity of billet is supposed to decrease along the distance from the entrance of the conical die, and it is expressed as:

$$\omega_z = \frac{z}{l}\omega_B \tag{2}$$

where $\omega_z$ is the angular velocity of the billet outer surface in the container, $\omega_B$ is the angular velocity of billet outer surface at the entrance of rotating die, $l$ is the axial twisting length of the billet inside container, $z$ is the distance of considered section from the entrance.

## 3. The UBM model for the extrusion force

*3.1. Velocity field*

*3.1.1. Velocity field inside the rotating die.* As shown in figure 3, based on the volume invariance, the velocity components caused by extrusion deformation can be expressed with a spherical velocity field by:

$$\dot{u}_\rho = \dot{u}_0 \frac{a^2}{\rho^2}\cos\theta \tag{3}$$

where the $\rho$ is the radial direction in the spherical coordinate system $(\rho,\varphi,\theta)$ with the origin at the apex of the cone.

IOP Conf. Series: Materials Science and Engineering 1270 (2022) 012075 doi:10.1088/1757-899X/1270/1/012075

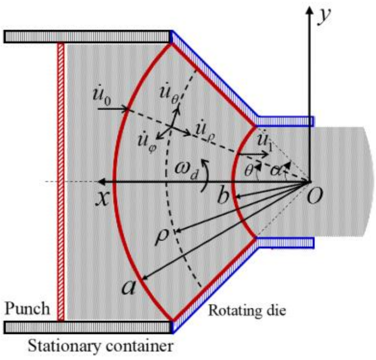


**Figure 3.** Compound spherical velocity field.

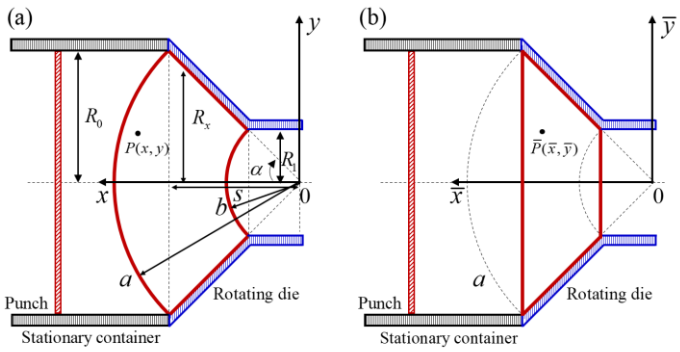


**Figure 4.** The schematic diagram of mapping relation; (a) deformation zone; (b) mapping zone.

The torsional angular velocities along the radial and axial directions are assumed quadratic and cubic function distribution, respectively, due to the radial and axial nonlinearity of torsional velocity in the deformation zone. In addition, considering its complexity, the shape of the deformation zone is mapped to a rectangular zone. As shown in figure 4, by establishing the torsional velocity field in the mapping zone, the torsional velocity field of the deformation zone is obtained according to the mapping relation, which can be expressed by:

$$\begin{aligned} \bar{x} &= \sqrt{x^2+y^2}\cos\alpha - b\cos\alpha \\ \bar{y} &= \frac{R_0}{R_x}\sqrt{x^2+y^2}\,\frac{y}{x}\cos\alpha \end{aligned} \tag{4}$$

where the $(\bar{x}, \bar{y})$ and $(x, y)$ are respectively the Cartesian coordinates for the mapping zone and for the deformation zone, and the $R_x$ is the radius of the billet at cross-section with coordinate $x$.

According to the torsional angular velocity assumptions, the mapping relationship, and the coordinate transformation from Cartesian to spherical coordinates, the torsional angular velocity in the deformation zone can be expressed as:

$$\begin{aligned} \omega &= k\omega_d + c_1(\rho\cos\alpha - b\cos\alpha) + c_2(\rho\cos\alpha - b\cos\alpha)^2 + c_3(\rho\cos\alpha - b\cos\alpha)^3 \\ &+ m_1\left(\frac{s\cos\alpha\sin\theta}{\cos^2\theta} - R_0\right) + m_2\left[\left(\frac{s\cos\alpha\sin\theta}{\cos^2\theta}\right)^2 - R_0{}^2\right] \end{aligned} \tag{5}$$

Therefore, the total velocity field in spherical coordinate system can be expressed as:

$$\dot{u}_\rho = \dot{u}_0\frac{a^2}{\rho^2}\cos\theta, \quad \dot{u}_\varphi = \omega\rho\sin\theta, \quad \dot{u}_\theta = 0 \tag{6}$$

The velocity difference between the rotating die and outer surface of billet can be expressed as:

$$\Delta v_{f1} = \sqrt{(\dot{u}_0\frac{a^2}{\rho^2}\cos\theta)^2 + \left[(\omega_d - \omega)\rho\sin\alpha\right]^2} \tag{7}$$

The velocity discontinuities along the boundaries $S_2$ and $S_3$ are coupled by extrusion and torsional velocity discontinuities, so the total velocity discontinuities can be expressed as:

$$\begin{aligned} \Delta v_{1-2} &= \sqrt{\left(\dot{u}_0\sin\theta\right)^2 + \left[(\omega_B - \omega_{1-2})a\sin\theta\right]^2} \\ \Delta v_{1-3} &= \sqrt{\left(\dot{u}_0\frac{a^2}{b^2}\sin\theta\right)^2 + \left[(\omega_C - \omega_{1-3})b\sin\theta\right]^2} \end{aligned} \tag{8}$$

where $\omega_{1-2}$ denotes the torsional angular velocity along the boundary $S_2$, $\omega_{1-3}$ denotes the torsional angular velocity along the boundary $S_3$, and the $\omega_{1-2}$, $\omega_{1-3}$ can be expressed as:

$$\omega_{1-2} = k\omega_d + c_1(a\cos\alpha - b\cos\alpha) + c_2(a\cos\alpha - b\cos\alpha)^2 + c_3(a\cos\alpha - b\cos\alpha)^3 + m_1\left(\frac{s\cos\alpha\sin\theta}{\cos^2\theta} - R_0\right) + m_2\left[\left(\frac{s\cos\alpha\sin\theta}{\cos^2\theta}\right)^2 - R_0^{\ 2}\right] \tag{9}$$

$$\omega_{1-3} = k\omega_d + m_1\left(\frac{s\cos\alpha\sin\theta}{\cos^2\theta} - R_0\right) + m_2\left|\left(\frac{s\cos\alpha\sin\theta}{\cos^2\theta}\right)^2 - R_0^{\ 2}\right| \tag{10}$$

*3.1.2. Velocity field inside the container*. For the billet inside the container, a cylindrical coordinate system $(z,r,\theta)$ is applied with the axis $z$ being the axis of the billet. As shown in figure 5, the velocity field can be expressed as:

$$\dot{u}_z = \dot{u}_0, \quad \dot{u}_r = \omega_z r, \quad \dot{u}_\theta = 0 \tag{11}$$

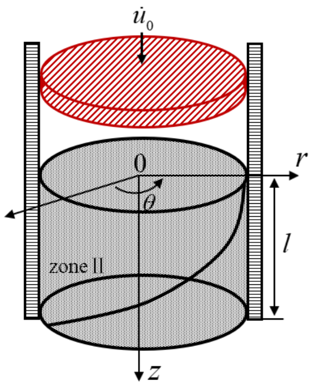


**Figure 5.** Deformation of billet inside the container

The velocity difference between the rotating die and outer surface of billet can be expressed as:

$$\Delta v_{f2} = \sqrt{(\dot{u}_0)^2 + (\omega_z R_0)^2} \tag{12}$$

*3.2. Deformation power*

The total deformation power of the billet can be expressed as:

$$\dot{W}_p = \int_V \sigma_Y \dot{\bar{\varepsilon}} \mathrm{d}V = \int_{V_1} \sigma_Y \dot{\bar{\varepsilon}}_1 \mathrm{d}V_1 + \int_{V_2} \sigma_Y \dot{\bar{\varepsilon}}_2 \mathrm{d}V_2 \tag{13}$$

where $\sigma_Y$ is the yield stress, $\dot{\bar{\varepsilon}}$ is the effective strain rate, $V_1$ and $V_2$ are the volume of the deformation zone I and II. For the billet inside the conical die, the strain rates can be expressed in the spherical coordinate system, as:

$$\begin{aligned}
&\dot{\varepsilon}_{\rho\rho}=\frac{\partial \dot{u}_\rho}{\partial \rho}=-2\dot{u}_0\frac{a^2}{\rho^3}\cos\theta\\
&\dot{\varepsilon}_{\theta\theta}=\frac{1}{\rho}\frac{\partial \dot{u}_\theta}{\partial \theta}+\frac{\partial \dot{u}_\rho}{\rho}=\dot{u}_0\frac{a^2}{\rho^3}\cos\theta\\
&\dot{\varepsilon}_{\varphi\varphi}=\frac{1}{\rho\sin\theta}\frac{\partial \dot{u}_\varphi}{\partial \varphi}+\frac{\partial \dot{u}_\rho}{\rho}+\frac{\partial \dot{u}_\theta}{\rho}\cot\theta=\dot{u}_0\frac{a^2}{\rho^3}\cos\theta\\
&\dot{\varepsilon}_{\rho\theta}=\frac{1}{2}(\frac{\partial \dot{u}_\theta}{\partial \rho}-\frac{\dot{u}_\theta}{\rho}+\frac{1}{\rho}\frac{\partial \dot{u}_\rho}{\partial \theta})=-\frac{1}{2}\dot{u}_0\frac{a^2}{\rho^3}\sin\theta\\
&\dot{\varepsilon}_{\theta\varphi}=\frac{1}{2}(\frac{1}{\rho\sin\theta}\frac{\partial \dot{u}_\theta}{\partial \varphi}+\frac{1}{\rho}\frac{\partial \dot{u}_\varphi}{\partial \theta}-\frac{\dot{u}_\varphi}{\rho}\cot\theta)\\
&=\frac{1}{2}\left[m_1 s\cos\alpha\frac{\sin\theta(2-\cos^2\theta)}{\cos^3\theta}+m_2 s^2\cos^2\alpha\frac{2\sin^2\theta\cos^2\theta+4\sin^4\theta}{\cos^5\theta}\right]\\
&\dot{\varepsilon}_{\varphi\rho}=\frac{1}{2}(\frac{\partial \dot{u}_\varphi}{\partial \rho}-\frac{\dot{u}_\varphi}{\rho}+\frac{1}{\rho\sin\theta}\frac{\partial \dot{u}_\rho}{\partial \varphi})\\
&=\frac{1}{2}\left[c_1\cos\alpha\rho\sin\theta+2c_2\cos^2\alpha(\rho-b)\rho\sin\theta+3c_3\cos^3\alpha(\rho-b)^2\rho\sin\theta\right]
\end{aligned} \tag{14}$$

It can be seen that the strain rate components caused by torsion has relation with the angle position $(\theta)$, and the effective strain rate $\dot{\bar{\varepsilon}}_1$ is expressed as:

$$\dot{\bar{\varepsilon}}_1=\sqrt{\frac{2}{3}\left[\dot{\varepsilon}_{\rho\rho}^2+\dot{\varepsilon}_{\theta\theta}^2+\dot{\varepsilon}_{\varphi\varphi}^2+2(\dot{\varepsilon}_{\rho\theta}^2+\dot{\varepsilon}_{\theta\varphi}^2+\dot{\varepsilon}_{\varphi\rho}^2)\right]} \tag{15}$$

For the billet within the container, the rotation of the die induces only a shear strain rate which can be expressed in the cylindrical coordinate system, as:

$$\begin{aligned}
&\dot{\varepsilon}_{\theta z}=\frac{1}{2}\left(\frac{\partial \dot{u}_\theta}{\partial z}+\frac{1}{r}\frac{\partial \dot{u}_r}{\partial \theta}\right)\\
&=\frac{\left[k\omega_d+c_1(a\cos\alpha-b\cos\alpha)+c_2(a\cos\alpha-b\cos\alpha)^2+c_3(a\cos\alpha-b\cos\alpha)^3\right]r}{2l}
\end{aligned} \tag{16}$$

The effective strain rate $\dot{\bar{\varepsilon}}_2$ is:

$$\dot{\bar{\varepsilon}}_2=\frac{2}{\sqrt{3}}\dot{\varepsilon}_{\theta z} \tag{17}$$

### *3.3. Friction losses*

The total friction losses can be expressed as:

$$\dot{W}_f=\int_S mK\Delta v\mathrm{d}S=\int_{S_1} mK\Delta\dot{u}_{f1}\mathrm{d}S_1+\int_{S_2} m_c K\Delta\dot{u}_{f2}\mathrm{d}S_2 \tag{18}$$

where $K$ is the yielding shear stress, assumed as $K=\sigma_Y/\sqrt{3}$, $m$ is the shear friction factor between the rotating die and billet, $m_c$ is the shear friction factor between the container and billet, $S_1$ and $S_2$ are the contact surfaces of billet with conical die and container, respectively.

According to the assumption (II), the twisting length of the billet in container is limited due to the friction between the container and billet. The twisting length $l$ can be expressed as in Ma [10]:

$$l=\frac{m}{m_c}\frac{1}{3\sin\alpha}\left[1-\left(\frac{R_1}{R_0}\right)^3\right] \tag{19}$$

*3.4. Power dissipation along velocity discontinuities*

The total dissipation power on the velocity discontinuity surfaces $S_2$ and $S_3$ can be expressed as:

$$\dot{W}_{S_{2,3}} = \int_S K\Delta v \mathrm{d}S = \int_{S_2} K\Delta\dot{u}_{1-2}\mathrm{d}S_2 + \int_{S_3} K\Delta\dot{u}_{1-3}\mathrm{d}S_3 \tag{20}$$

*3.5. External power*

The external power is provided by the punch and the rotating die, and can be expressed as:

$$J^* = q\pi R_0^2\dot{u}_0 + M\omega_d \tag{21}$$

where $q$ denotes the averaged punch pressure, $M$ and $\omega_d$ are respectively the torque and angular velocity of the rotating die driven by the external motor.

For a material point $P$ on the contact surface between the billet and the rotating die, as shown in the figure 6, the velocity $v$ can be decomposed into two components, $v_\rho$ and $v_\varphi$, which can be expressed as:

$$\begin{aligned} v_\rho &= \dot{u}_0 \frac{a^2}{\rho^2}\cos\alpha \\ v_\varphi &= \left[(1-k)\omega_d + c_1(\rho\cos\alpha - b\cos\alpha) + c_2(\rho\cos\alpha - b\cos\alpha)^2 + c_3(\rho\cos\alpha - b\cos\alpha)^3\right]\rho\sin\alpha \end{aligned} \tag{22}$$

It is assumed that friction vector $mK$ on the point $P$ is opposite to the direction of relative motion, correspondingly, it is also decomposed into components in the radial and circumferential directions, $mK\sin\gamma$ and $mK\cos\gamma$, where $\gamma$ is the angle between $v_\varphi$ and $v$, as:

$$\tan\gamma = \frac{v_\rho}{v_\varphi} \tag{23}$$

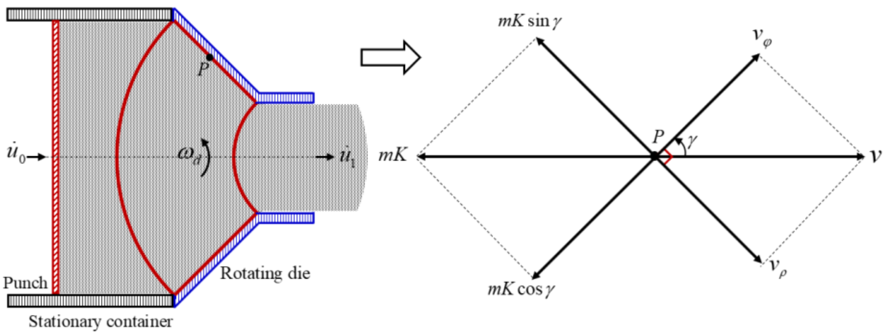


**Figure 6.** Shear stress distribution of the billet on the outer surface of the point.

Since the $mK\cos\gamma$ provides the torque to move point $P$ along the circumferential direction, the total torque can be expressed as:

$$M = \int_{S_1} mK\cos\gamma\rho\sin\alpha\mathrm{d}S \tag{24}$$

Substituting eq. (22) and (23) into eq. (24) yields:

$$M = \frac{2}{\sqrt{3}}\pi m\sigma_Y\sin^2\alpha\int_b^a \frac{\Delta\omega\rho^3\sin\alpha}{\sqrt{(\dot{u}_0\frac{a^2}{\rho^2}\cos\alpha)^2 + (\Delta\omega\rho\sin\alpha)^2}}\mathrm{d}\rho \tag{25}$$

*3.6. Extrusion force*

According to the upper bound theorem, an inequality for the extrusion force is established as:

$$\frac{q}{\sigma_Y} \leq \frac{\dot{W}_p + \dot{W}_f + \dot{W}_{S2,3} - M\omega_d}{\pi R_0^{\ 2} \dot{u}_0 \sigma_Y} \tag{26}$$

where the undetermined parameters $m_1$, $m_2$, $c_1$, $c_2$, $c_3$ and $k$ are involved. The extrusion force is obtained by minimizing $q$ through optimizing these undetermined parameters.

## 4. Results and discussions

The procedure to solve the extrusion force was coded in MATLAB, and the results is validated by the finite element (FEM) simulations.

### *4.1. The finite element modeling*

To validate the UBM model, a finite element model for the torsion-extrusion was established by using DEFORM-3D, in which the geometrical dimensions and flow properties of the material were the same as in the upper bound analysis. The model is shown in figure 7, where the punch, container and the rotating die were assumed as rigid body.

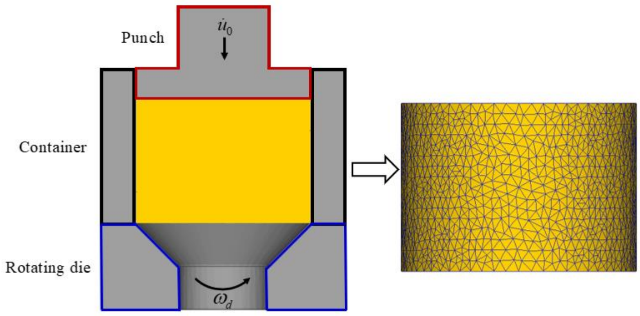


**Figure 7.** The finite element model.

The extruded material is 6 wt% $TiB_2$/7075 Al composite with an initial diameter of 28.28 mm and length of 30 mm. The stress-strain relationship is obtained by hot compressions. The initial temperatures are respectively 623 K for the billet, 298 K for the punch, and 553 K for the other two tools. The heat transfer coefficients are assumed 11 N/K/s/mm between billet and the tools, and 0.02 N/K/s/mm between billet and air. The extrusion speed is 1.0 mm/s, the rotating angular velocity of conical die is 1 rad/s.

### *4.2. Comparison of relative extrusion force*

In the upper bound method, the force is usually expressed by pressure, as in eq. (26). To compare the extrusion force obtained by UBM and FEM, the dimensionless pressure is defined by dividing the pressure by the flow stress. The comparison is shown in figure. 8. It can be seen that, with the increase of the shear friction factor of the rotating die, the relative extrusion force obtained from the UBM and FEM presents a tendency of decreasing. Since the friction between the rotating die and billet is the driving force for the torsional deformation of the billet, the torsion brings deformation energy to the billet that makes the extrusion force decrease, and such a conclusion was also pointed out by Maciejewski [11]. The comparison shows an acceptable discrepancy for the extrusion force obtained by UBM and FEM, which verifies the accuracy of the UBM model.

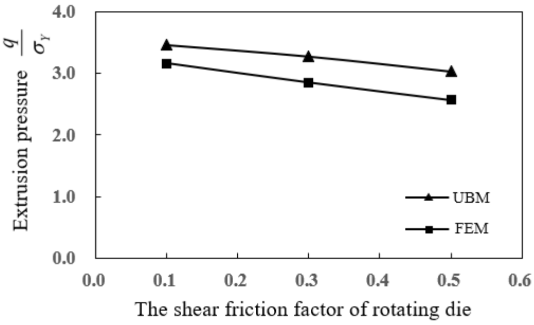


**Figure 8.** The comparison of relative extrusion force.

Meanwhile, the influences of extrusion ratio and semi-die angle on the extrusion force are investigated as well. Figure 9 shows the variation of relative extrusion pressure with (a) the semi-cone angle of die and (b) the extrusion ratio. In these figures, the influence of the rotating velocity is also compared. Due to the friction and the length of the deformation zone varied with the die angle, the relative extrusion pressure decreases firstly and then increases with the increasing of the die angle. In all the cases, the extrusion pressure is decreased with the assistance of the torsion.

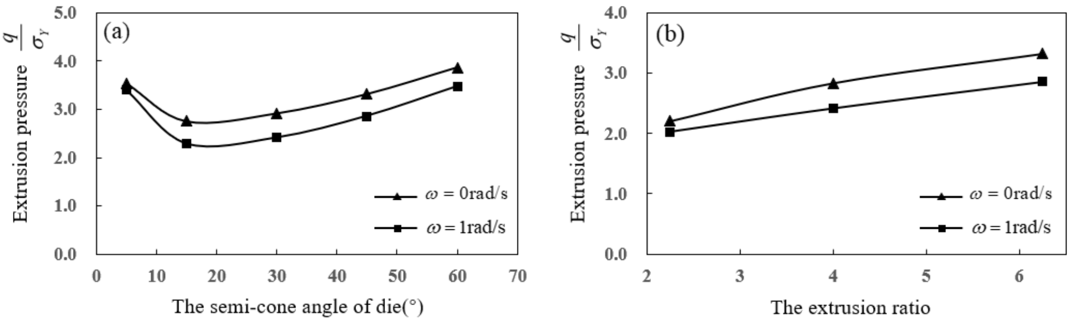


**Figure 9.** The variation of relative extrusion force; (a) the semi-cone angle of die; (b) the extrusion ratio.

### *4.3. Analysis of the metal flow*

The UBM is also able to output the information of metal flow. Taking the case shown in 4.1 as the example, the semi-cone angle of die is 45°, and the shear friction factors of the billet surface with the rotating die and the container are assumed as 0.3. The unknown parameters $(m_1, m_2, c_1, c_2, c_3, k)$ involved in the velocity field are assigned with initial values $(0,0,0,0,0,1)$, then through optimizing the eq. (26) by using particle swarm optimization, the optimized values for these variables are obtained and they are $(0.0427, -0.00177, -0.0965, 0.00729, 0.0000625, 0.815)$. Therefore, the torsional angular velocity in the deformation zone shown in figure 3 can be expressed as:

$$\begin{aligned}\omega = {} & 0.815 - 0.0682(\rho - 10) + 0.00365(\rho - 10)^2 + 0.0000221(\rho - 10)^3 \\ & + 0.427\left(\frac{\sin\theta}{\cos^2\theta} - \sqrt{2}\right) - 0.177\left(\frac{\sin^2\theta}{\cos^4\theta} - 2\right)\end{aligned} \tag{27}$$

According to eq. (6), the circumferential velocity in the deformation zone can be expressed as:

$$\dot{u}_{\varphi} = \begin{bmatrix} 0.815 - 0.0682(\rho - 10) + 0.00365(\rho - 10)^2 + 0.0000221(\rho - 10)^3 \\ +0.427\left(\dfrac{\sin\theta}{\cos^2\theta} - \sqrt{2}\right) - 0.177\left(\dfrac{\sin^2\theta}{\cos^4\theta} - 2\right) \end{bmatrix} \rho \sin\theta \tag{28}$$

Figure 10 shows the velocity distribution of billet inside the rotating die. As shown in figure 10(a) and (c), the rotating angular velocity of billet gradually decreases from the outer surface to the center in the radial direction, which is because that the billet rotation is driven by the friction between the rotating die and billet. Meanwhile, the angular velocity of billet along the axis direction gradually decreases from the exit to the entrance of conical die. Figure 10(b) and (d) show the contour of the rotating velocity with respect of $\rho$ and $\theta$.

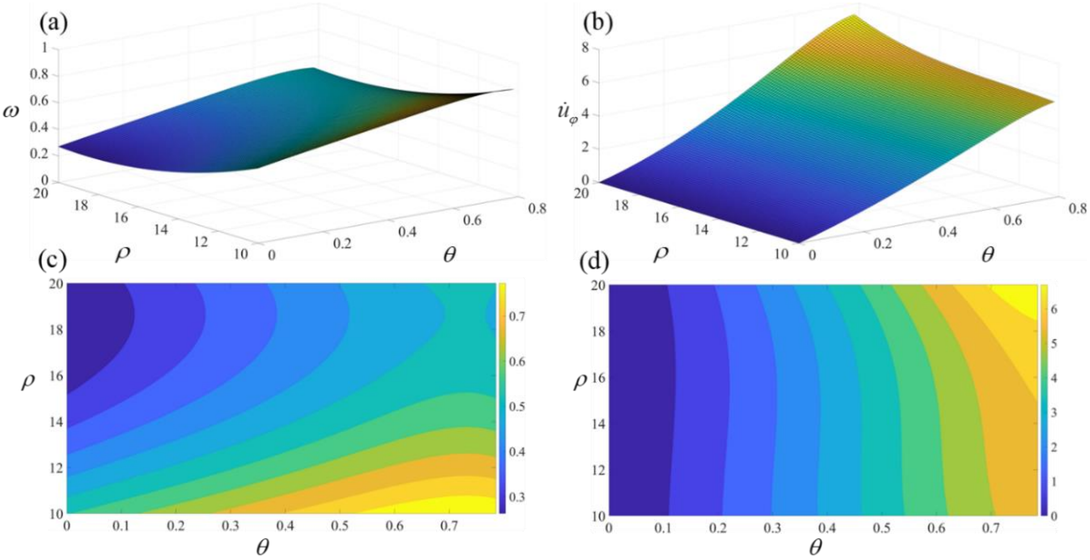


**Figure 10.** The velocity distribution of billet inside the rotating die; (a) the angular velocity; (b) the circumferential velocity; (c) the contour of angular velocity; (d) the contour of circumferential velocity.

## 5. Conclusion

An upper bound model is proposed to predict the extrusion force in torsion extrusion process, in which several undetermined parameters were involved in the assumed velocity field and they are determined by minimizing the extrusion force. The method was verified by the finite element simulation. Meanwhile, the influences of various process parameters on the extrusion force are analyzed. The conclusion can be drawn as follows.

(1) The kinematically admissible velocity field was constructed by involving several undetermined parameters, especially for the torsional velocity, which makes the velocity field able to represent complex deformation mode that exists in the torsional extrusion process.

(2) The upper bound model can reasonably predict the extrusion force under various processing parameters including the friction factor, reduction ratio and die angle.

(3) The extrusion force can be significantly decreased with the assistance of torsion deformation, especially, when the rotating die has a large friction.

## References

[1] Valiev R Z, Islamgaliev R K and Alexandrov I V 2000 Bulk nanostructured materials from severe plastic deformation *Prog Mater Sci* **45**(2) 103-89

IOP Conf. Series: Materials Science and Engineering 1270 (2022) 012075 doi:10.1088/1757-899X/1270/1/012075

[2] Estrin Y and Vinogradov A 2013 Extreme grain refinement by severe plastic deformation: A wealth of challenging science *Acta Mater* **61**(3) 782-817
[3] Sabirov I, Kolednik O and Valiev R Z 2005 Equal channel angular pressing of metal matrix composites: effect on particle distribution and fracture toughness *Acta Mater* 2005 **53**(18) 4919-30
[4] Zhilyaev A P and Langdon T G 2008 Using high-pressure torsion for metal processing: Fundamentals and applications *Prog Mater Sci* **53**(6) 893-79
[5] Saito Y, Utsunomiya H and Tsuji N 1999 Novel ultra-high straining process for bulk materials—development of the accumulative roll-bonding (ARB) process *Acta Mater* **47**(2) 579-83
[6] Mishra R S and Ma Z Y 2005 Friction stir welding and processing *Mater Sci Eng* R 2005 **50**(1-2) 1-78
[7] Zhao S, Zhang H and Cui Z 2020 Particle dispersion and grain refinement of in-situ TiB2 particle reinforced 7075 Al composite processed by elliptical cross-section torsion extrusion *J Alloys Compd* 834 155136
[8] Brovman M J 1987 Steady forming processes of plastic materials with their rotation *Int J of Mech Sci* **29**(7) 483-89
[9] Ma X, Barnett M R and Kim Y H 2004 Forward extrusion through steadily rotating conical dies. Part I: experiments *Int J of Mech Sci* **46**(3) 449-64
[10] Ma X, Barnett M R and Kim Y H 2004 Forward extrusion through steadily rotating conical dies Part II: theoretical analysis *Int J of Mech Sci* **46**(3) 465-89
[11] Maciejewski J and Mróz Z 2008 An upper-bound analysis of axisymmetric extrusion assisted by cyclic torsion *J Mater Process Technol* **206**(1-3) 333-44

**Acknowledgements**
This research work was financially supported by the National Natural Science Foundation of China under the project Nos. 52075328.